Available online at www.sciencedirect.com

ScienceDirect

Procedia Engineering 14 (2011) 1439–1446

Procedia Engineering

www.elsevier.com/locate/procedia

The Twelfth East Asia-Pacific Conference on Structural Engineering and Construction

Inverse Technique for Deformational Analysis of Concrete Beams with Ordinary Reinforcement and Steel Fibers

G. KAKLAUSKAS[a], V. GRIBNIAK[b], and D. BACINSKAS

Department of Bridges and Special Structures, Vilnius Gediminas Technical University, Lithuania

Abstract

The smeared crack model, extensively applied in numerical analysis of reinforced concrete structures, is based on use of average stress-average strain constitutive relationships. This model is very effective for deformation analysis of steel fiber reinforced concrete (SFRC) members as cracking deformations of such members are restrained by fibers. One of the most critical points in the theory of SFRC is quantifying residual tension stresses for a cracked section. The purpose of the present study is to apply the inverse technique for determining residual stresses of SFRC in tension. The proposed method aims at deriving average stress-average strain relationships of cracked tensile concrete using test data of SFRC flexural members reinforced with steel bars. The paper reports results of the experimental program consisting of five beams reinforced in the tension zone with three 10 mm bars in diameter. The beams had different contents of fibers, i.e. 0, 0.3, 0.5, 1.0 and 1.5% by volume. The proposed inverse technique has been applied to the test data and average stress-strain relationships in tension were derived for each beam. It has been shown that residual stresses increase with growing amount of fiber until the content reaches 1% of the element volume. Under this limit, the efficiency of fiber increases proportionally to its content, whereas, its influence becomes less significant above the limit.

Keywords: Reinforced concrete, inverse analysis, steel fibers, residual stresses, deformations.

[a]Presenter: Email: Gintaris.Kaklauskas@vgtu.lt
[b]Corresponding author: Email: Viktor.Gribniak@vgtu.lt

1877–7058 © 2011 Published by Elsevier Ltd. Open access under CC BY-NC-ND license.
doi:10.1016/j.proeng.2011.07.181

1 INTRODUCTION

In last decades, fiber reinforcement is widely used as additive for concrete mixture for production of modern structures. Fiber reinforcement significantly improves service properties of concrete. Its influence on concrete member is more effective than bar reinforcement, as tensile deformations are restrained in the whole volume of tensile zone, whereas, tensile deformations in a reinforced concrete (RC) member are restrained in the specific interaction area of reinforcement and concrete.

One of the most critical points in the theory of SFRC (Campione and Mangiavillano 2008, Brandt 2008, Radtke et al. 2010) is quantifying residual tension stresses for a cracked section. Present practices of composing stress-strain diagrams in tension are based on experimental results of small SFRC specimens. However, these tests require relatively sophisticated experimental equipment (based on strain regulated load application) mainly available at research centers only. The purpose of the present study is to apply inverse technique for determining residual stresses of SFRC in tension.

Smeared crack approach is extensively applied in numerical analysis of SFRC structures. This model is very effective for analysis of SFRC members as fibers reduce discrete cracking phenomena by smearing out cracking deformations. *Kaklauskas* and *Ghaboussi* (2001) have formulated the principles of the inverse technique for determining stress-strain tension-stiffening relationship using test data of RC flexural members. Modifications of the technique have been introduced by *Gribniak* (2009) to improve the computational efficiency by reducing the influence of scatter of test data points of moment-curvature diagrams on the analysis results.

Present study is dedicated to the experimental and analytical investigation of deformations and cracking of SFRC beams. The paper reports results of the experimental program consisting of five beams, which were reinforced in the tension zone with three 10 mm bars in diameter. The beams had different contents of fibers, i.e. 0, 0.3, 0.5, 1.0 and 1.5% by volume. Based on the inverse procedure, average stress-strain relationships for concrete in tension were derived from the moment-curvature diagrams of the experimental beams.

2 INVERSE ANALYSIS OF THE FLEXURAL MEMBERS

This section presents a numerical procedure for deriving an average stress-average strain tension-stiffening relationship from a moment-curvature diagram of concrete beams with ordinary reinforcement and steel fibers. The analysis procedure is based on formulae of strength of materials extended to application of the *layer* section model and material diagrams. The following approaches and assumptions have been adopted:

1) smeared crack approach; 2) linear strain distribution within the depth of the section implying perfect bond between concrete and reinforcement; 3) all concrete fibers in the tension zone follow a uniform stress-strain tension-stiffening law.

2.1 Direct technique

The *direct* technique uses a simple iterative technique of deformational analysis of composite members based on the *layer* section model (Kaklauskas 2004). Let us consider a doubly reinforced concrete member subjected to pure bending. A cross-section for such member is presented in Figure 1a. The member's cross-section is divided into horizontal layers corresponding to either concrete or reinforcement (see Figure 1b). Thickness of the reinforcement layer is taken from the condition of the equivalent area. The analysis needs to assume material laws for reinforcement and concrete schematically shown in Figures 1f and 1g.

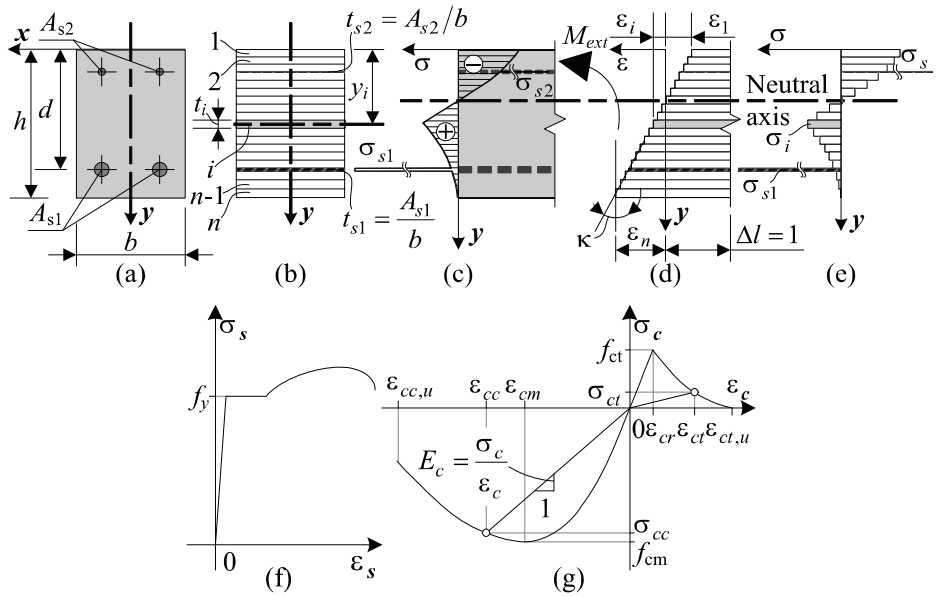

Figure 1: *Layer* section model of RC section (a)–(e) and a constitutive relationships for reinforcement steel (f) and concrete (g).

Curvature κ and strain ε_i at any layer *i* (see Figure 1d) can be calculated by the formulae:

$$\kappa = M_{ext}/(IE); \quad \varepsilon_i = M_{ext}(y_i - y_{RC})/(IE); \quad y_{RC} = SE/(AE); \quad AE = \sum_{i=1}^{n} b_i t_i E_i;$$
$$SE = \sum_{i=1}^{n} b_i t_i y_i E_i; \quad IE = \sum_{i=1}^{n} \left[b_i t_i^3/12 + b_i t_i (y_i - y_{RC})^2 \right] E_i; \quad E_i = \sigma_i/\varepsilon_i . \tag{1}$$

Here M_{ext} is the external bending moment; *AE*, *SE* and *IE* are the area, the first and the second moments of the area multiplied by the secant modulus; *n* is the total number of layers; b_i and t_i are the width and thickness of the *i*-th layer, respectively; y_i is the distance of the *i*-th layer from the top edge of the section (see Figure 1b). For the given strains and constitutive laws (see Figures 1d and 1c), stresses and corresponding secant modulus are calculated. The analysis is performed iteratively until convergence of the secant modulus at each layer is reached. Figures 1d and 1e illustrate strain and stress distributions within the *layer* section model.

2.2 Inverse technique

Differently from direct analysis which results in the prediction of structural response using the specified constitutive model, inverse analysis aims at determining parameters of the model based on the response of the structure. This Section sketches a solution of the *inverse* problem discussing major aspects only. *Kaklauskas* and *Ghaboussi* (2001) formulated the principles of the *inverse* technique for deriving average stress-strain relationship of concrete in tension using test data of RC flexural members. For given experimental moment-curvature curve, a stress-strain relationship was defined from the equilibrium equations of the axial forces and the bending moments. The *layer* section model (see Figure 1b) was employed for computation of the internal forces. The analysis was performed via load (bending moment) increments. The two equilibrium equations were solved for each loading stage yielding a

solution for the coordinate of neutral axis and the concrete stress in the extreme tension fiber. Since the extreme fiber had the largest strain, other tension fibers of concrete had smaller strains falling within the portion of the stress-strain diagram which had already been determined (see the third assumption). The average stress-strain relationship of concrete in tension was progressively derived assuming the portions obtained from the previous increments.

Present research employs the inverse technique modified by *Gribniak* (2009). Modifications were aiming at improving the computational efficiency and reducing the influence of scatter of test data points of moment-curvature diagrams on the analysis results. The analysis is based on the *direct* technique (see Section 2.1.) and the above mentioned concept of progressive calculation of stress-strain relationship for the extreme tension fiber of concrete. The assumption of uniform stress-strain tension-stiffening law for different layers facilitates reducing the dimension of the solution, i.e. a single non-linear equation is solved. For given load increment, initial value of the secant deformation modulus of stress-strain relationship is assumed and curvature is calculated. If the calculated curvature differs from the experimental value more than the assumed tolerance, the needed secant deformation modulus is derived using classical methods of the iterative analysis.

The flow chart of the inverse technique is displayed in Figure 2. Based on geometrical parameters of the cross-section, the *layer* section is composed. The stress-strain material laws for steel and compressive concrete are assumed. Computations are performed iteratively via bending moment increments. At each moment increment i, initial value of secant deformation modulus of stress-strain relationship under derivation is assumed equal to zero. Such assumption makes the calculation procedure more stabile (Gribniak 2009). Curvature $\kappa_{th,i}$ is calculated by the *direct* analysis. If the agreement between the calculated and the experimental curvature $\kappa_{obs,i}$ is not within the assumed tolerance Δ ($\left|\delta_{i,k}\right| = \left|\left(\kappa_{th,i}/\kappa_{obs,i}\right)-1\right| > \Delta$), i.e. Condition **1** is not fulfilled (see Figure 2), the analysis is repeated using the hybrid *Newton-Raphson & Bisection* procedure (Gribniak 2009) until Condition **2** is satisfied. At each iteration k, the secant deformation modulus $E_{i,k}$ is calculated. If the solution is found, i.e. Condition **1** is satisfied, the obtained value of $E_{i,k}$ is fixed and used for the next load increments. If the limit iteration number is exceeded ($k > N = 30$), the present load step is discarded and the analysis is moved to the successive load step. The calculation is terminated when the ultimate loading step is reached (Condition **3**). The analysis results in the derived average stress-strain tension-stiffening relationship.

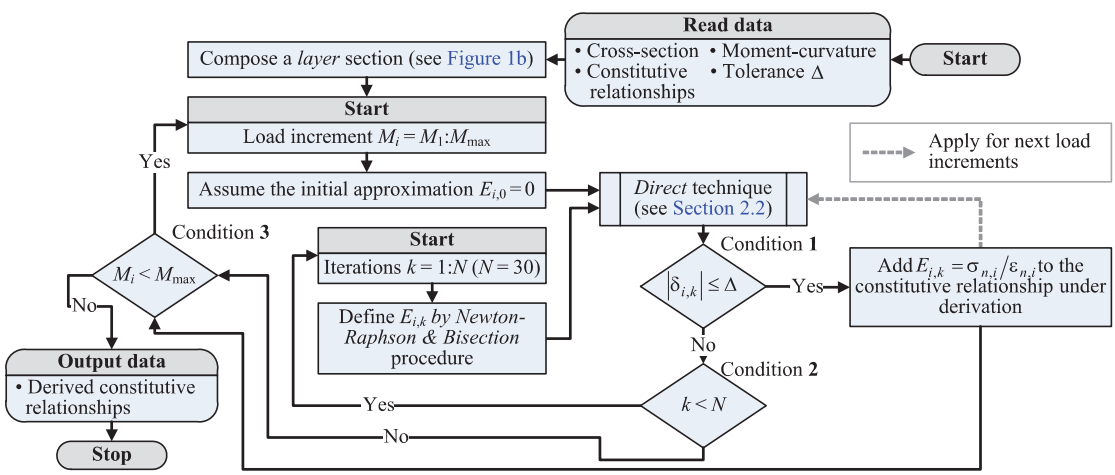

Figure 2: Flow chart of the procedure for solving inverse problem.

3 EXPERIMENTAL INVESTIGATION

This Section reports results of the test program performed by the authors. Deformation behavior of concrete beams with ordinary reinforcement and steel fibers was studied. The program consisted of five beams, having the same amount of bar reinforcement but different contents of fibers.

3.1 Description of test beams

All the beams were of rectangular cross-section; with nominal length 3280 mm (span 3000 mm). The beams were tested under a four-point bending scheme with 1 m shear spans. All beams were reinforced in the tension zone with three bars of tensile reinforcement 10 mm in diameter with reinforcement ratio 0.3%. The beams had different contents of fibers *f*, i.e. 0, 0.3, 0.5, 1.0 and 1.5% by volume. Main parameters of the experimental beams are listed in Table 1.

3.2 Material properties

All beams were cast using steel formwork. The beams were unmolded in about 2-3 days after casting. The specimens were cured at average relative humidity 73% and temperature 20 °C. The ordinary Portland cement and crushed aggregate (16 mm maximum nominal size) were used. Concrete mix proportion was taken to be uniform for all experimental specimens: 1 m^3 contained 905 kg of sand, 936 kg of rough aggregate and 400 kg of cement. Water/cement and aggregate/cement ratio by weight were taken as 0.42 and 2.97, respectively. *DUOLOC* fibers (aspect ratio: 55 mm / 1 mm) were used.

In order to determine material properties of concrete, twelve $\varnothing 150 \times 400$ mm cylinders, fifteen $100 \times 100 \times 400$ mm and five $300 \times 280 \times 350$ mm prisms were cast. The latter specimens were cast in the moulds of the test beams and were used for shrinkage measurements. Compressive strength and deformation tests were performed at test day. Three cylinders and three $100 \times 100 \times 400$ mm prisms were tested. The latter specimens were used for deriving the stress and strain relationship.

$\varnothing$10 mm deformed bars of mild steel were used for the main reinforcement. Three samples of the bars were tested and several lengths were weighed to check the nominal diameter. The stresses and modulus of elasticity are based on the nominal diameters. The yield strength was 560 MPa. The elastic modulus was obtained to be 203 GPa.

3.3 Tests of beams

As noted above, the free shrinkage deformations of 280×300×350 mm concrete prisms (fragments of the test beams) were measured. After unmolding, their ends were isolated with polyester film. The measured free shrinkage strains ε_{sh} are presented in Table 1.

The loading scheme and the gauge positioning are shown in Figure 3. The test specimens were loaded with a 100 kN hydraulic jack in a stiff testing frame. The tests were performed with small increments (2 kN) and paused for short periods (about 2 minutes) to take readings of gauges and to measure crack development. On average, the experimental loading took 60-80 increments with total test duration of 3 hours. The testing equipment acting on the beam weighed 232 kg. The latter summed up with the beam's own weight has in the mid-span induced a 3.5 kNm bending moment.

Concrete surface strains were measured throughout the length of the pure bending zone on a 200 mm gauge length, using mechanical gauges. As shown in Figure 3 (view 'A'), four continuous gauge lines were located at different depths. The two extreme gauge lines were placed along the top and the bottom reinforcement whereas two other lines were located 60 mm off these lines. To measure the deflections,

the linear variable differential transducers (L_1-L_8, see Figure 3) were placed beneath the soffit of each of the beam at the load position.

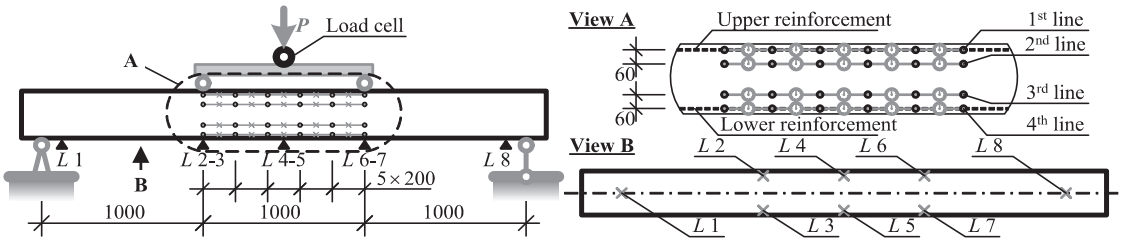

Figure 3: Loading scheme and experimental set-up of the beams.

Table 1: Main characteristics of experimental beams

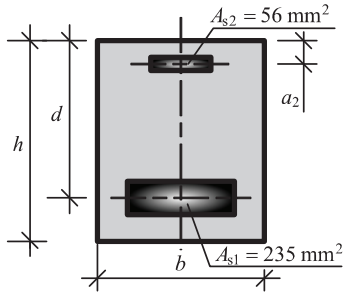

Beam	h	b	d	a_2	Age	f_{cu}	ε_{sh}	f
	mm				days	MPa	μm/m	%
S3-2-3	298	284	271	32	47	50.9	–210.9	–
S3-2-7F	298	284	271	20	49	44.6	–205.3	0.29
S3-1-F05	302	278	278	29	170	55.6	–311.2	0.47
S3-1-F10	300	279	276	23	161	48.0	–335.5	1.02
S3-1-F15	300	279	272	26	159	52.2	–315.7	1.46

4 DERIVING TENSION-STIFFENING RELATIONSHIPS FROM TEST RESULTS

Moment-curvature diagrams of the beams are shown in Figure 4a. This figure shows the curvatures obtained from both the average longitudinal strains and the deflections over the pure bending zone. The technique for deriving such diagrams is presented in (Gribniak et al. 2009). Good agreement of the diagrams can be stated. Further analysis will be based on the diagrams derived from the average strains. As seen in Figure 4a, the beams with larger amounts of fiber reinforcement had higher stiffness. The authors have proposed the numerical procedure for deriving *free-of-shrinkage* moment-curvature relationships (Kaklauskas et al. 2008). This procedure was applied to test data of the beams. The derived *free-of-shrinkage* moment-curvature diagrams are presented in Figure 4b.

The average stress-strain relationships of SFRC in tension were derived by the *inverse* technique using the *free-of-shrinkage* moment-curvature diagrams. The normalized average stress-strain diagrams are shown in Figure 5, where $f_{ct,EC2}$ and ε_{cr} are the tensile strength and the cracking strain of concrete, respectively. These parameters were calculated according to the *Eurocode 2*.

It should be noted that the residual stresses in the diagrams presented in Figure 5 consist of stresses corresponding to the tension-stiffening effect and the stresses due to fiber interaction with concrete. This figure clearly indicates that the residual stresses increase with growing amount of fiber until the content reaches 1% of the element volume. Under this limit, the efficiency of fiber increases proportionally to its content, whereas, its influence is less significant above the limit.

It is important that the average stress-strain relationships obtained in this study might be incorporated directly into the smeared finite element codes (for example *ATENA* software) as SFRC material model.

This is a major advantage of the proposed technique in respect to the commonly accepted approach based on the tests of four-point bending of notched or un-notched prisms.

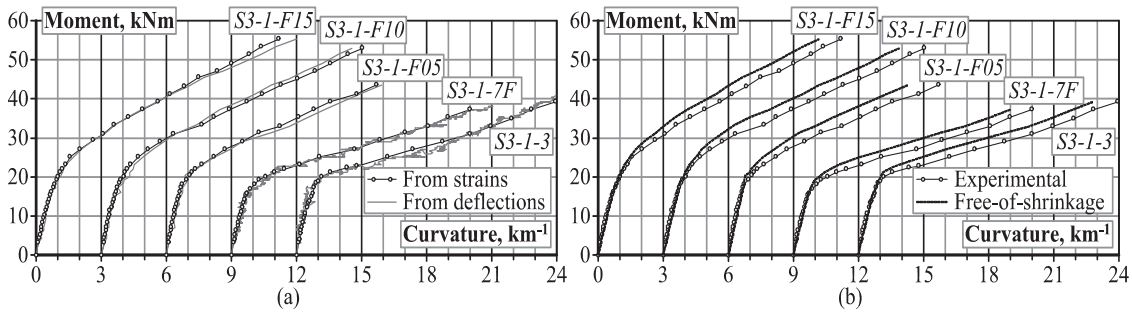

Figure 4: Curvatures of the test beams: obtained from deflections and longitudinal strains measured at the surface (a) and derived eliminating shrinkage effect (b).

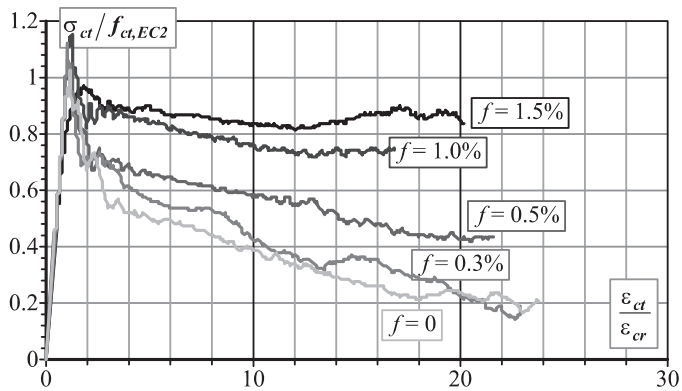

Figure 5: Average stress-average strain relationships of SFRC in tension.

5 CONCLUDING REMARKS

The paper deals with experimental and theoretical investigation of cracking and deformation behavior of concrete beams with ordinary reinforcement and steel fibers. Experimental results have been reported on five lightly reinforced concrete beams (about 0.3%) with different contents of fibers, i.e. 0, 0.3, 0.5, 1.0 and 1.5% by volume. Based on the inverse technique developed by the authors, average stress-strain relationships of SFRC in tension were derived from test data of the beams. Two main conclusions were made: 1) Influence of steel fiber on the stress-strain relationships is proportional until fiber content reaches 1% of the element volume. 2) The proposed technique for analysis of SFRC beams is capable of deriving average stress-strain relationships of SFRC applicable for numerical modeling. Further investigations are needed for developing a versatile stress-strain law.

Acknowledgements

The authors gratefully acknowledge the financial support provided by the *Research Council of Lithuania* (research project *MIP–126/2010*). The second author also expresses his gratitude to the *Research Council of Lithuania* for the Postdoctoral fellowship.

References

[1] Brandt AM (2008). Fibre reinforced cement-based (FRC) composites after over 40 years of development in building and civil engineering. Composite Structures. 86(1-3), pp. 3-9.

[2] Campione G and Mangiavillano ML (2008). Fibrous reinforced concrete beams in flexure: Experimental investigation, analytical modelling and design considerations. Engineering Structures. 30(11), pp. 2970-2980.

[3] Gribniak V (2009). Shrinkage influence on tension-stiffening of concrete structures. Ph. D. thesis, Vilnius Gediminas Technical University, Lithuania. (Full-text access at http://www.dart-europe.eu/full.php?id=182160).

[4] Gribniak V, Kaklauskas G, and Bacinskas D (2009). Experimental investigation of shrinkage influence on tension stiffening of RC beams. Proceedings of Creep, Shrinkage and Durability of Concrete and Concrete Structures (ConCreep 8), Ise-Shima, Japan, pp. 571-577.

[5] Kaklauskas G (2004). Flexural layered deformational model of reinforced concrete members. Magazine of Concrete Research. 56(10), pp. 575-584.

[6] Kaklauskas G and Ghaboussi J (2001). Stress-strain relations for cracked tensile concrete from RC beam tests. ASCE Journal of Structural Engineering. 127(1), pp. 64-73.

[7] Kaklauskas G, Gribniak V, Bacinskas D (2008). Free of shrinkage tension stiffening relationships derived from RC beam tests. Proceedings of Sixth International Conference Analytical Models and New Concepts in Concrete and Masonry Structures (AMCM‘2008), Lodz, Poland, pp. 329-330.

[8] Radtke FKF, Simone A, and Sluys LJ (2010). A computational model for failure analysis of fibre reinforced concrete with discrete treatment of fibres. Engineering Fracture Mechanics. 77(4), pp. 597-620.